EFFECTS OF CHEMICAL REACTION, THERMAL RADIATION, INTERNAL HEAT GENERATION, SORET AND DUFOUR ON CHEMICALLY REACTING MHD BOUNDARY LAYER FLOW OF HEAT AND MASS TRANSFER PAST A MO VING VERTICAL PLATE WITH SUCTION/INJECTION

Supported by tetfund TERTIARY EDUCATION TRUST FUND

E.O. Titiloye[1], A.O. Adesanya[2], A.O. Ibrahim[3] and P.O. Olanrewaju[4]

[1]Department of Mathematics, University of Ilorin, Kwara State, Nigeria

[2]Department of Mathematics & Computer Science, Elizade University, Ilara Mokin, Ondo State, Nigeria

[3]Department of Mathematical Sciences, Oduduwa University, Ipetumodu, Osun State, Nigeria, West Africa

[4]Department of Mathematics & Statistics, Federal University Wukari, Taraba State, Nigeria

Corresponding author: oladapo_anu@yahoo.ie

Abstract: In the present analysis, we study the two-dimensional, steady, incompressible electrically conducting, laminar free convection boundary layer flow of a continuously moving vertical porous plate in a chemically reactive medium in the presence of transverse magnetic field, thermal radiation, chemical reaction, internal heat generation and Dufour and Soret effect with suction/injection. The governing nonlinear partial differential equations have been reduced to the coupled nonlinear ordinary differential equations by the similarity transformations. The problem is solved numerically using shooting techniques with the sixth order Runge-Kutta integration scheme. Comparison between the existing literature and the present study were carried out and found to be in excellent agreement. The influence of the various interesting parameters on the flow and heat transfer is analyzed and discussed through graphs in detail. The values of the local Nusselt number, Skin-friction and the Sherwood number for different physical parameters are also tabulated. Comparison of the present results with known numerical results is shown and a good agreement is observed.

Keywords: Thermal radiation, magneto-hydrodynamics (MHD), soret and Dufour, free convection.

Introduction

Boundary-layer flows over a moving plate are of great importance in view of their relevance to a wide variety of technical applications, particularly in the manufacture of fibers in glass and polymer industries. The first and foremost work regarding the boundary-layer behavior in moving surfaces in quiescent fluid was considered by Sakiadis (1961).Subsequently, many researchers (Crane, 1970; Gupta and Gupta, 1977; Caragher and Crane, 1982; Danberg and Fansler, 1976; Chakrabarti and Gupta, 1979; Vajravelu, 1986; Dutta, 1986; Lee and Tsai, 1990) worked on the problem of moving or stretching plates under different situations. In the boundary-layer theory, similarity solutions are found to be useful in the interpretation of certain fluid motions at large Reynolds numbers. Similarity solutions often exist for the flow over semi-infinite plates and stagnation point flow for two dimensional, axi-symmetric and three dimensional bodies. In some special cases, when there is no similarity solution, one has to solve a system of non-linear partial differential equations (PDEs). For similarity boundary-layer flows, velocity profiles are similar. But, this kind of similarity is lost for non-similarity flows (Wanous and Sparrow, 1965; Catherall and Williams, 1965; and Sparrow *et al.*, 1970; Sparrow and Yu, 1971; Massoudi, 2001). Obviously, the non-similarity boundary-layer flows are more general in nature and more important not only in theory but also in applications.

The flow of an incompressible fluid past a moving surface has several engineering applications. The aerodynamic extrusion of plastic sheets, the cooling of a large metallic plate in a cooling bath, the boundary layer along a liquid film in condensation process and a polymer sheet or filament extruded continuously from a die, or a long thread traveling between a feed roll and a wind-up roll are the examples of practical applications of a continuous flat surface. In certain dilute polymer solution (such as 5.4% of polyisobutylene in cetane and 0.83% solution of ammonium alginate in water (Erickson *et al.*, 1966; Crane, 1970), the viscoelastic fluid flow occurs over a stretching sheet.

Convective flow in porous media has been widely studied in the recent years due to its wide applications in engineering as postaccidental heat removal in nuclear reactors, solar collectors, drying processes, heat exchangers, geothermal and oil recovery, building construction, etc. (Nield and Bejan, 2006; Ingham and Pop, 2005; Vafai, 2005; Vadasz, 2008, etc.). It is well known that conventional heat transfer fluids, including oil, water, and ethylene glycol mixture are poor heat transfer fluids, since the thermal conductivity of these fluids plays an important role on the heat transfer coefficient between the heat transfer medium and the heat transfer surface. An innovative technique for improving heat transfer by using ultra fine solid particles in the fluids has been used extensively during the last several years. The free-convection flow with thermal radiation and mass transfer past a moving vertical porous plate was investigated by Makinde (2005) whilst laminar free convection flow from a continuously-moving vertical surface in a thermally-stratified non-Darcy high-porosity medium was presented by Anwar *et al.* (2008). The problem of magneto-hydrodynamics natural convection about a vertical impermeable flat plate can be found in Sparrow and Cess (1961), Yih (1999) studied the free convection effect on MHD coupled heat and mass transfer of a moving permeable vertical surface. Alan and Rahman (2006), examined Dufour and Soret effects on mixed convection flow past a vertical porous flat plate with variable suction embedded in a porous medium for a hydrogen-air mixture as the non-chemical reacting fluid pair. Olanrewaju (2010) examined Dufour and Soret Effects of a Transient Free Convective Flow with Radiative Heat Transfer Past a Flat Plate Moving through a Binary Mixture. Recently, Ibrahim and Makinde (2010) studied the combined effects of wall suction and magnetic field on boundary layer flow with

heat and mass transfer over an accelerating vertical plate. The present communication considers the Effects of thermal radiation, chemical reaction, internal heat generation, Soret and Dufour on chemically reacting MHD boundary layer flow of heat and mass transfer past a moving vertical plate with suction/injection. It investigates numerically the effects of heat and mass transfer in a hydromagnetic boundary layer flow of a moving vertical porous plate with uniform heat generation, chemical reaction, thermal radiation, and magnetic strength field with Dufour and Soret in the presence of suction/injection. By using scaling transformations, the set of governing equations and the boundary conditions are reduced to non-linear ordinary differential equations with appropriate boundary conditions. Furthermore, the similarity equations are solved numerically by using shooting technique with sixth-order Runge-Kutta integration scheme. Numerical results of the local skin friction coefficient, the local Nusselt number and the Sherwood number as well as the velocity, temperature and concentration profiles are presented for different physical parameters.

Governing equations

We consider the steady free convective heat and mass transfer flow of a viscous, incompressible and electrically conducting fluid past a moving vertical plate with suction/injection in the presence of thermal diffusion (Soret) and diffusion-thermo (Dufour) effects (see Fig. 1) The non-uniform transverse magnetic field B_o is imposed along the y-axis. The induced magnetic field is neglected as the magnetic Reynolds number of the flow is taken to be very small. It is also assumed that the external electric field is zero and the electric field due to polarization of charges is negligible. The temperature and the concentration of the ambient fluid are T_∞ *and* C_∞, and those at the surface are $T_w(x)$ *and* $C_w(x)$, respectively.

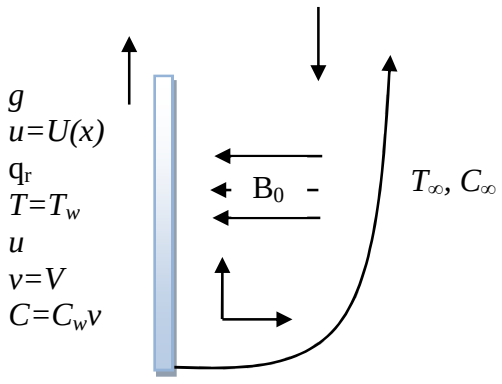

Fig.1: Physical configuration and coordinate system

It is also assumed that the pressure gradient, viscous and electrical dissipation are neglected. The fluid properties are assumed to be constant except the density in the buoyancy terms of the linear momentum equation which is approximated according to the Boussinesq's approximation. Under the above assumptions, the boundary layer form of the governing equation can be written as (see Kafoussias and Williams (1995))

$$\frac{\partial u}{\partial x}+\frac{\partial v}{\partial y}=0 \quad \ldots\ldots\ldots\ldots\ldots\ldots (1)$$

$$u\frac{\partial u}{\partial x}+v\frac{\partial u}{\partial y}=\nu\frac{\partial^2 u}{\partial y^2}+g\beta_T(T-T_\infty)+g\beta_C(C-C_\infty)-\frac{\sigma B_o^2}{\rho}u \quad \ldots (2)$$

$$u\frac{\partial T}{\partial x}+v\frac{\partial T}{\partial y}=\alpha\frac{\partial^2 T}{\partial y^2}+\frac{D_m k_T}{c_s c_p}\frac{\partial^2 C}{\partial y^2}-\frac{\alpha_1}{\rho}\frac{\partial q_r}{\partial y}+Q(T-T_\infty) \quad \ldots\ldots\ldots (3)$$

$$u\frac{\partial C}{\partial x}+v\frac{\partial C}{\partial y}=D_m\frac{\partial^2 C}{\partial y^2}+\frac{D_m k_T}{T_m}\frac{\partial^2 T}{\partial y^2}-R^*(C-C_\infty) \quad \ldots\ldots (4)$$

The boundary conditions for Eqs. (1)-(4) are expressed as;

$$v=V, u=Bx, T=T_w=T_\infty+ax, C=C_w=C_\infty+bx \ \text{at} \ y=0, \quad \ldots\ldots\ldots (5)$$
$$u\to 0, T\to T_\infty, C\to C_\infty \ \text{as} \ y\to\infty,$$

where B is a constant, a and b denotes the stratification rate of the gradient of ambient temperature and concentration profiles, (u, v) are the velocity components in x- and y- directions, respectively, T is the temperature, β_T is the volumentric coefficient of thermal expansion, α_1 is the thermal diffusivity, g is the acceleration due to gravity, υ is the kinematic viscosity, D_m is the coefficient of diffusion in the mixture, C is the species concentration, σ is the electrical conductivity, B_o is the externally imposed magnetic field in the y-direction, k_T is the thermal-diffusion ratio, c_s is the concentration susceptibility, c_p is the specific heat at constant pressure and T_m is the mean fluid temperature. Using the Rosseland approximation, the radiative heat flux in the y-direction is given by Sparrow and Cess (1978),

$$q_r = -\frac{4\sigma^*}{3K'}\frac{\partial T^4}{\partial y}, \quad \ldots\ldots\ldots\ldots\ldots (6)$$

where σ^* *and* K' are the Stefan-Boltzmann constant and the mean absorption coefficient, respectively. Following Makinde and Ogulu (2008), we assume that the temperature differences within the flow are sufficiently small so that the T^4 can be expressed as a linear function after using Taylor series to expand T^4about the free stream temperature T_∞ and neglecting higher-order terms. This result is the following approximation:

$$T^4 \approx 4T_\infty^3 T-3T_\infty^4. \quad \ldots\ldots\ldots\ldots\ldots (7)$$

Using (6) and (7) in (3), we obtain

$$\frac{\partial q_r}{\partial y}=-\frac{16\sigma^*}{3K}\frac{\partial T^4}{\partial y}. \quad \ldots\ldots\ldots\ldots\ldots (9)$$

We nondimensionalize (1)-(4) using the following transformations:

$$\eta=\sqrt{\frac{B}{\upsilon}}y,\ F(\eta)=\frac{\psi}{x\sqrt{B\upsilon}},\ \theta(\eta)=\frac{T-T_\infty}{T_w-T_\infty},\ \phi(\eta)=\frac{C-C_\infty}{C_w-C_\infty},\quad \ldots\ldots(10)$$

where ψ is the stream function defined by $u=\partial\psi/\partial x$ and $v=-\partial\psi/\partial y$ in order to satisfy to satisfy the continuity equation (1).Where $F(\eta)$ is a dimensionless stream function, $\theta(\eta)$ is a dimensionless temperature of the fluid in the boundary layer region, $\phi(\eta)$is a dimensionless species concentration of the fluid in the boundary layer region and η is the similarity variable. The velocity components u and v are respectively obtained as follows

$$u=\frac{\partial\psi}{\partial y}=xBF',\ v=-\frac{\partial\psi}{\partial x}=-\sqrt{B\upsilon}F,\quad \ldots\ldots\ldots\ldots(11)$$

Where $F_w=\dfrac{V}{\sqrt{B\upsilon}}$ is the dimensionless suction velocity.

Following eqs.(10) and (11), the partial differential equations (2)-(4) are transformed into local similarity equations as follows:

$$F'''+FF''-(F'+M)F'+G_r\theta+G_c\phi=0\quad \ldots\ldots(12)$$

$$\theta''[1+\frac{4}{3}Ra]+\Pr(F\theta'-F'\theta)+\Pr\ Du\ \phi''+\Pr\ \alpha\theta=0\quad \ldots(13)$$

$$\phi''+Sc(F\phi'-F'\phi)+ScSr\ \theta''-Sc\,\gamma\phi=0,\ \ldots..(14)$$

where primes denote differentiation with respect to η. The appropriate flat, free convection boundary conditions are also transformed into the form,

$$F'=1,\ F=-F_w,\ \theta=1,\phi=1\ at\ \eta=0\quad \ldots\ldots\ldots..(15)$$
$$F'=0,\ \theta=0,\ \phi=0\ as\ \eta\to\infty,$$

Where: $M=\dfrac{\sigma B_o^2}{\rho B}$ is the magnetic parameter,

$\Pr=\dfrac{\upsilon}{\alpha}$ is the Prandtl number,

$Sc=\dfrac{\upsilon}{D_m}$ is the Schmidt number,

$G_r=\dfrac{g\beta_T(T_w-T_\infty)}{xB^2}$ is the local temperature Grashof number,

$G_c=\dfrac{g\beta_c(C_w-C_\infty)}{xB^2}$ is the local concentration Grashof number,

$D_u=\dfrac{D_m k_T(C_w-C_\infty)}{c_s c_p(T_w-T_\infty)}$ is the Dufour number,

$S_r=\dfrac{D_m k_T(T_w-T_\infty)}{T_m(C_w-C_\infty)\upsilon}$ is the Soret number.

$\alpha = Q/B\alpha_1$ is the internal heat generation

$\gamma = \upsilon R^*/B^2$ is the chemical reaction parameter

The quantities of physical interest in this problem are local skin friction, the local Nusselt number, and the local Sherwood number.

Computational procedure

The set of Eqs. (12)-(14) together with the boundary conditions (15) have been solved numerically by applying Nachtsheim-Swigert shooting iteration technique along with Runge-Kutta sixth-order integration method. From the process of numerical computation, the skin-friction coefficient, the local Nusselt number and the local Sherwood number, which are respectively proportional to $f''(0),-\theta'(0)\ and\ -\phi'(0),$ are also sorted out and their numerical values are presented in a tabular form. The computations have been performed by a program which usesa symbolic and computational computer language MAPLE (see Heck (2003)). A step size of $\Delta\eta$ = 0.001 is selected to be satisfactory for a convergence criterion of 10^{-7} in nearly all cases. The value of y_∞ is found to each iteration loop by the assignment statement $\eta_\infty = \eta_\infty + \Delta\eta$. The maximum value of η_∞, to each group of parameters, *Pr*, *Sc*, *Sr*, D_u, *M*, *Ra*, G_T, G_C, *K* , *S*, $\alpha$and $\gamma$is determined when the values of unknown boundary conditions at η = 0 do not change to successful loop with error less than 10^{-7}.

Results and Discussion

In order to get a clear insight of the physical problem, the velocity, temperature and concentration have been discussed by assigning numerical values to the parameters encountered in the problem. To be realistic, the values of the embedded parameters were chosen following Ibrahim & Makinde [20] Attention is focused on positive values of the buoyancy parameters i.e. Grashof number $G_T > 0$ (which corresponds to the cooling problem) and solutal Grashof number $G_C > 0$ (which indicates that the chemical species concentration in the free stream region is less than the concentration at the boundary surface) and the volumentric heat generation/absorption parameter. The cooling problem is often encountered in engineering applications. In Table 1, comparison is made for some fixed parameters and there is a perfect agreement with Ibrahim and Makinde (2005) which is a special case of ours. We went further in table 2 to generate the skin friction coefficient, Nusselt number and the Sherwood number for some embedded parameters value in the flow model. Here, the values of Dufour number and Soret number are chosen so that their product is constant provided that the mean temperature is also kept constant.

It is clearly seen that an increase in the parameters M, Sc, Pr, Ra, Sr and γ leads to an increase in the skin-friction at the wall plate while increase in parameters Gr, Gc, f_w, Du and α decreases the skin-friction at the wall surface. Similarly, the Nusselt number coefficient increases at the wall plate when Gr, G_C, f_w, Pr and Ra increases while it decreases at the wall plate when parameters M, Sr, Du, α and γ increases. It is interesting to note that Sherwood number at the wall plate increases with increase in Gc, M, Sc, Pr, α and γ decreases with other parameters embedded in the flow model.

Table 1: Computation showing comparison with Ibrahim & Makinde (2010) of $F''(0), \theta'(0)$ and $\phi'(0)$ for various values of embedded flow parameters for *Pr* = 0.72, *Sr* = 0, *Du* = 0, *α* = 0, *Ra* = 0, and γ = 0

Gr	Gc	M	F_w	Sc	Present $-F''(0)$	Present $-\theta'(0)$	Present $-\phi'(0)$	Ibrahim & Makinde (2010) $-F''(0)$	Ibrahim & Makinde (2010) $-\theta'(0)$	Ibrahim & Makinde (2010) $-\phi'(0)$
0.1	0.1	0.1	0.1	0.62	0.8890854	0.7965304	0.7254766	0.888971	0.7965511	0.7253292
0.5	0.1	0.1	0.1	0.62	0.69603619	0.83787782	0.76585079	0.695974	0.8379008	0.7658018
1.0	0.1	0.1	0.1	0.62	0.47509316	0.87526944	0.80202587	0.475058	0.8752835	0.8020042
0.1	0.5	0.1	0.1	0.62	0.68702142	0.84207706	0.77016532	0.686927	0.8421370	0.7701717
0.1	1.0	0.1	0.1	0.62	0.45778202	0.88182384	0.80871749	0.457723	0.8818619	0.8087332
0.1	0.1	1.0	0.1	0.62	1.26462533	0.70938977	0.64116350	1.264488	0.7089150	0.6400051
0.1	0.1	3.0	0.1	0.62	1.86838864	0.58541218	0.52519379	1.868158	0.5825119	0.5204793
0.1	0.1	0.1	1.0	0.62	0.57074524	0.56010990	0.52730854	0.570663	0.5601256	0.5271504
0.1	0.1	0.1	3.0	0.62	0.27515400	0.29557231	0.29025308	0.275153	0.2955702	0.2902427
0.1	0.1	0.1	0.1	0.78	0.89351757	0.79373969	0.83398390	0.893454	0.7936791	0.8339779
0.1	0.1	0.1	0.1	2.62	0.91236953	0.78489176	1.65041891	0.912307	0.7847840	1.6504511

Table 2: Computation showing $F''(0)$, $\theta'(0)$ and $\phi'(0)$ for various values of embedded flow parameters

Gr	*Gc*	*M*	*Fw*	*Sc*	*Pr*	*Sr*	*Du*	*α*	γ	Ra	$-F''(0)$	$-\theta'(0)$	$-\phi'(0)$
0.1	0.1	0.1	0.1	0.62	0.72	0.1	0.03	1	1	0.1	0.6857050	-2.521404	1.202090
0.5	0.1	0.1	0.1	0.62	0.72	0.1	0.03	1	1	0.1	0.4766934	-0.165968	1.172184
1.0	0.1	0.1	0.1	0.62	0.72	0.1	0.03	1	1	0.1	0.2377260	0.1739780	1.183749
0.1	0.5	0.1	0.1	0.62	0.72	0.1	0.03	1	1	0.1	0.5501700	-2.331515	1.205999
0.1	1.0	0.1	0.1	0.62	0.72	0.1	0.03	1	1	0.1	0.3819476	-2.102049	1.210881
0.1	0.1	1.0	0.1	0.62	0.72	0.1	0.03	1	1	0.1	0.9925398	-5.877328	1.251050
0.1	0.1	1.5	0.1	0.62	0.72	0.1	0.03	1	1	0.1	1.1493539	-7.687298	1.279015
0.1	0.1	0.1	1.0	0.62	0.72	0.1	0.03	1	1	0.1	0.4673465	-1.810943	0.898195
0.1	0.1	0.1	2.0	0.62	0.72	0.1	0.03	1	1	0.1	0.3516448	-0.705366	0.662772
0.1	0.1	0.1	-0.1	0.62	0.72	0.1	0.03	1	1	0.1	0.7321387	-2.927027	1.286751
0.1	0.1	0.1	-1.0	0.62	0.72	0.1	0.03	1	1	0.1	1.2234841	-2.573560	1.618071
0.1	0.1	0.1	0.1	0.78	0.72	0.1	0.03	1	1	0.1	0.6662407	-2.810866	1.358596
0.1	0.1	0.1	0.1	2.62	0.72	0.1	0.03	1	1	0.1	0.6773186	-2.854431	2.457772
0.1	0.1	0.1	0.1	0.62	1.0	0.1	0.03	1	1	0.1	0.6754098	-3.056807	1.223527
0.1	0.1	0.1	0.1	0.62	3.0	0.1	0.03	1	1	0.1	0.7792231	-2.695652	1.230853
0.1	0.1	0.1	0.1	0.62	7.0	0.1	0.03	1	1	0.1	0.8675786	-1.037836	1.169757
0.1	0.1	0.1	0.1	0.62	0.72	0.4	0.03	1	1	0.1	0.6742893	-2.765831	1.389394
0.1	0.1	0.1	0.1	0.62	0.72	2.0	0.03	1	1	0.1	0.7156069	-2.783903	2.392893
0.1	0.1	0.1	0.1	0.62	0.72	0.1	0.15	1	1	0.1	0.6648644	-2.841222	1.212446
0.1	0.1	0.1	0.1	0.62	0.72	0.1	0.20	1	1	0.1	0.6641262	-2.872122	1.213809
0.1	0.1	0.1	0.1	0.62	0.72	0.1	0.03	2	1	0.1	0.0934791	-18.42139	1.669504
0.1	0.1	0.1	0.1	0.62	0.72	0.1	0.03	2.2	1	0.1	-0.052747	-23.56778	1.816335
0.1	0.1	0.1	0.1	0.62	0.72	0.1	0.03	1	2	0.1	0.668837	-2.784687	1.439166
0.1	0.1	0.1	0.1	0.62	0.72	0.1	0.03	1	3	0.1	0.6705748	-2.795142	1.636884
0.1	0.1	0.1	0.1	0.62	0.72	0.1	0.03	1	1	1.0	0.6656195	-2.093633	1.182462
0.1	0.1	0.1	0.1	0.62	0.72	0.1	0.03	1	1	3.0	0.6874687	-1.425462	1.162069

Velocity profiles

The effects of various thermophysical parameters on the fluid velocity are illustrated in Figs. 2 to 6. Fig. 2 depicts the effect of magnetic strength parameter M on the fluid velocity and we observed a decrease in the fluid velocity as parameter*M* increases. This is because an increase in the magnetic strength parameter stabilizes the fluid motion or flow. Fig. 3 depicts the influence of suction parameter *Fw* decreases the fluid velocity while injection increases the fluid velocity. It is interesting to note that increasing thermal and solutal Grashof numbers (Gr, G_C) increases the fluid velocity (Figs. 4 and 5). In figure 6, we display the graph of velocity profiles with various values of energy generation parameter α against spanwise coordinate η. It is interesting to note that increasing the parameter α bring an increase in the fluid velocity.

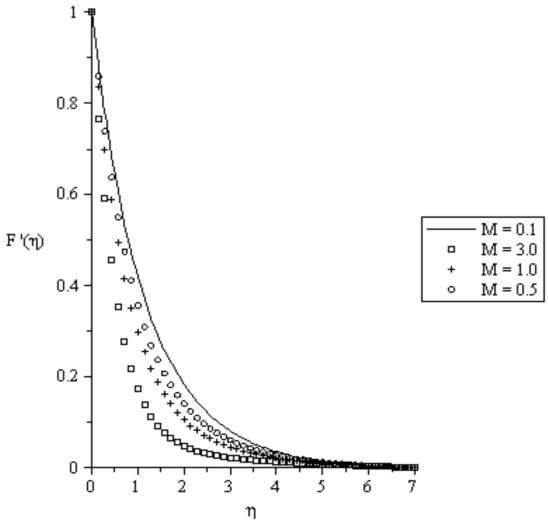

Fig. 2: Velocity profiles for Gr = Gc = Sr = F_w = γ = α = Ra = 0.1, Pr = 0.72, Sc = 0.62, Du = 0.03.

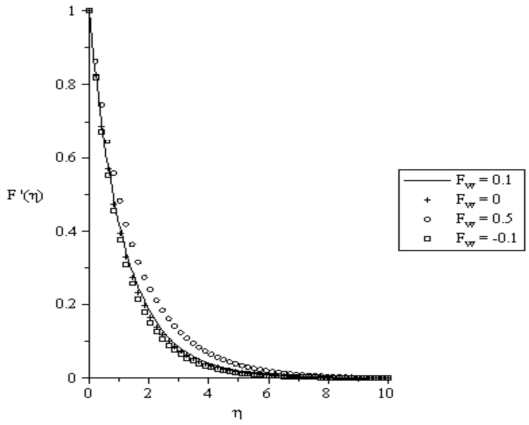

Fig 3: Velocity profiles for Gr = Gc = Sr = γ = α = Ra = M = 0.1, Pr = 0.72, Sc = 0.62, Du = 0.03.

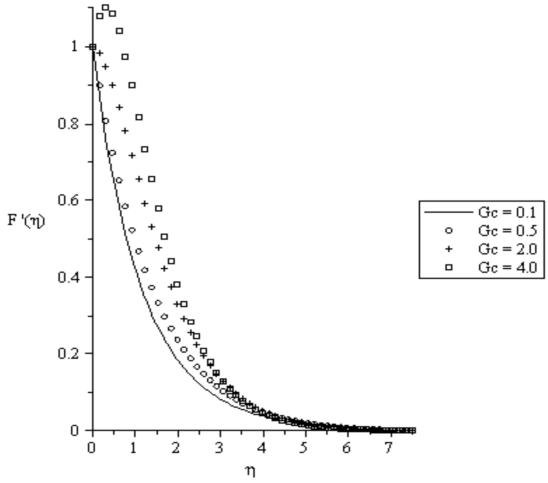

Fig. 4: Velocity profiles for *Gr* = F_w = *Sr* = *γ* = *α* = *Ra* = *M* = 0.1, *Pr* = 0.72, *Sc* = 0.62, *Du* = 0.03.

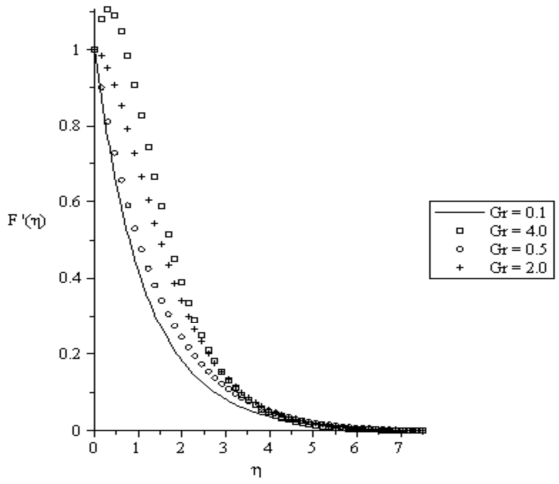

Fig. 5: Velocity profiles for *Gc* = F_w = *Sr* = *γ* = *α* = *Ra* = *M* = 0.1, *Pr* = 0.72, *Sc* = 0.62, *Du* = 0.03.

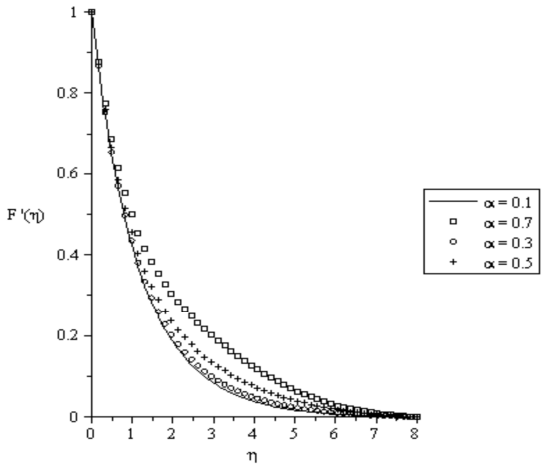

Fig. 6: Velocity profiles for Gc = Gr = F_w = γ = Ra = Sr = M = 0.1, Sc = 0.62, Du = 0.03, Pr = 0.72.

Temperature profiles

The influences of various embedded parameters on the fluid temperature are illustrated in Figs. 7 to 14. Fig. 7 depicts the graph of temperature against spanwise coordinate η for various values of magnetic strength parameter M. It is interesting to note that the thermal boundary layer thickness increases as M increases. In Fig. 8, it is seen that suction decreases the thermal boundary layer thickness while injection decreases the thermal boundary layer thickness. It is interesting to note that the thermal boundary layer thickness increases as the thermal and the solutal Grashof numbers increases (Figs. 9 and 10). Fig. 12 depicts the curve of temperature against spanwise coordinate η for various values of Prandtl number *Pr*. It is clearly seen that increases in the Prandtl number decreases the temperature profile and thereby decreases the thermal boundary layer thickness. At high Prandtl fluid has low velocity, which in turn also implies that at lower fluid velocity the specie diffusion is comparatively lower and hence higher specie concentration is observed at high Prandtl number. In Fig. 11, there is a slight increase in the thermal boundary layer thickness when the Dufour number is increased. Increase in the value of the internal heat generation parameter and radiation parameter (α, Ra) increases the thermal boundary layer thickness (Figs. 13 and 14).

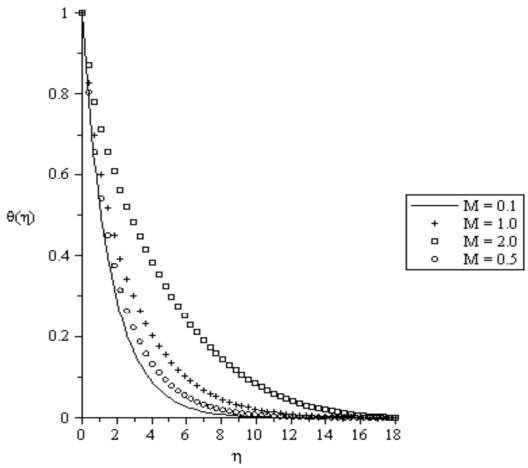

Fig. 7: Temperature profiles for Gr = Gc = Sr = F_w = γ = α = Ra = 0.1, Pr = 0.72, Sc = 0.62, Du = 0.03.

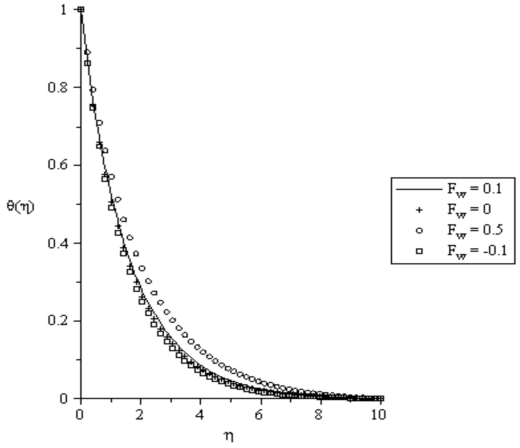

Fig. 8: Temperature profiles for Gr = Gc = Sr = γ = α = Ra = M = 0.1, Pr = 0.72, Sc = 0.62, Du = 0.03.

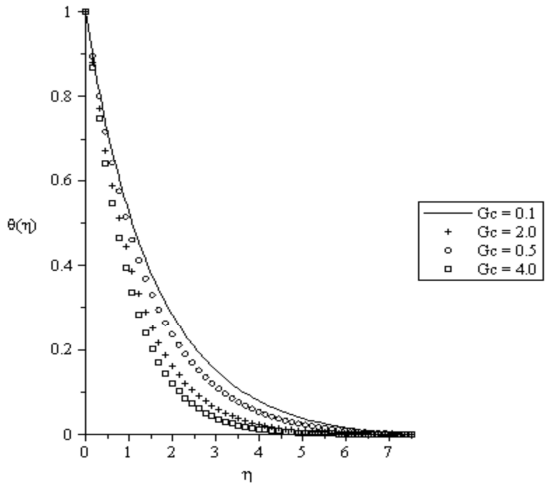

Fig. 9: Temperature profiles for Gr = F_w = Sr = γ = α = Ra = M = 0.1, Pr = 0.72, Sc = 0.62, Du = 0.03.

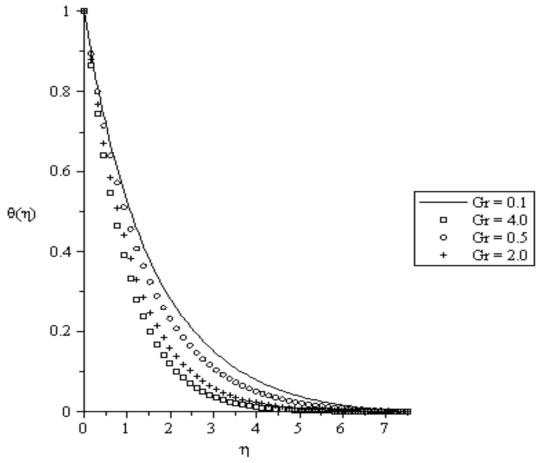

Fig. 10: Temperature profiles for Gc = F_w = Sr = γ = α = Ra = M = 0.1, Pr = 0.72, Sc = 0.62, Du = 0.03.

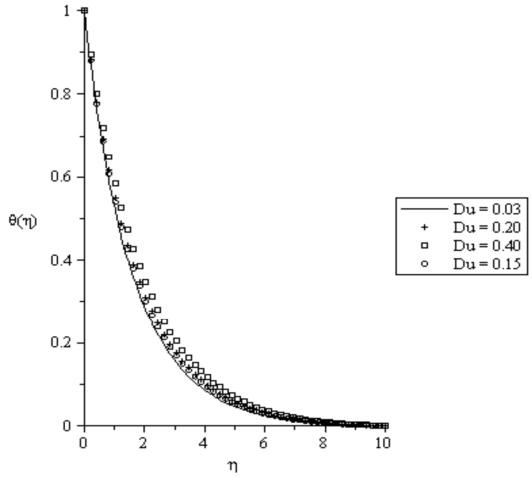

Fig. 11: Temperature profiles for Gc = Gr = F_w = Sr = γ = α = Ra = M = 0.1, Pr = 0.72, Sc = 0.62.

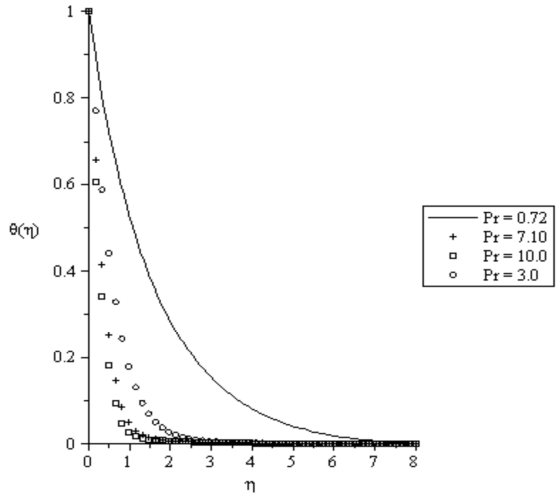

Fig. 12: Temperature profiles for Gc = Gr = F_w = γ = α = Ra = Sr = M = 0.1, Sc = 0.62, Du = 0.03.

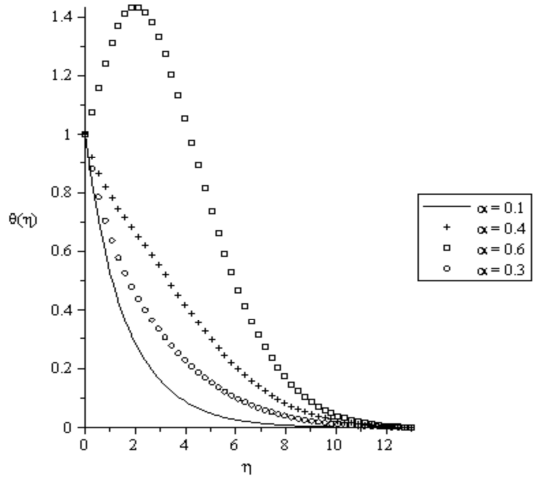

Fig. 13: Temperature profiles for Gc = Gr = F_w = γ = Ra = Sr = M = 0.1, Sc = 0.62, Du = 0.03, Pr = 0.72.

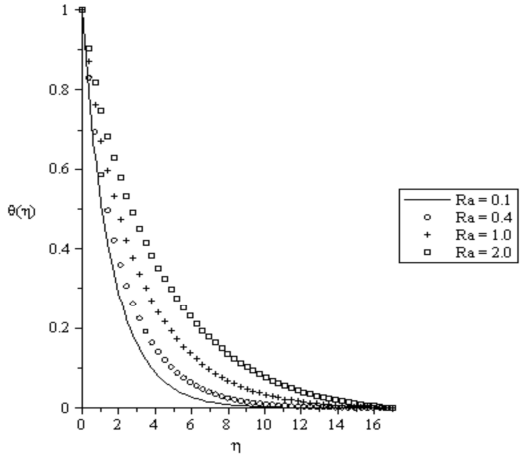

Fig. 14: Temperature profiles for Gc = Gr = F_w = α = γ = Sr = M = 0.1, Sc = 0.62, Du = 0.03, Pr = 0.72.

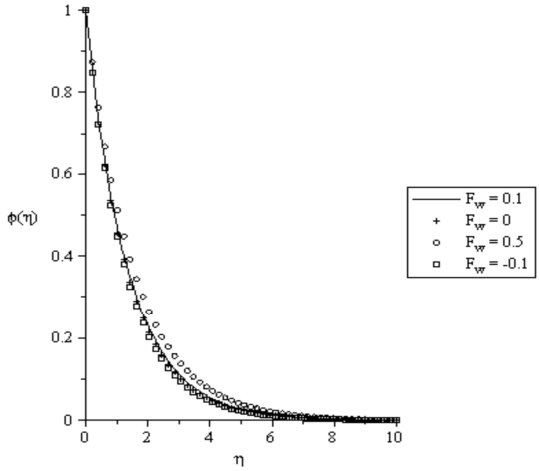

Fig. 16: Concentration profiles for Gr = Gc = Sr = γ = α = Ra = M = 0.1, Pr = 0.72, Sc = 0.62, Du = 0.03.

Concentration profiles

The effects of various thermophysical parameters on the fluid concentration are illustrated in Figs. 15 to 22. Fig. 16 reflects that with increase in magnetic strength parameter Mincreases the fluid concentration. It is clearly seen that suction and injection has similar effects with velocity and temperature profiles. In Figs. 17 and 18, it is clearly seen that the thermal and solutal Grashof numbers is to decrease the concentration boundary layer thickness. Fig. 19 depicts the curve of the concentration profile against spanwise coordinate η for various values of Schmitz number Sc. We notice that Sc is to decrease the concentration boundary layer thickness across the boundary.

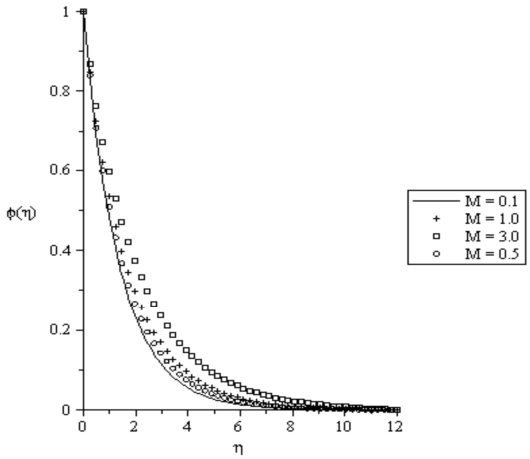

Fig. 15: Concentration profiles for Gr = Gc = Sr = F_w = γ = α = Ra = 0.1, Pr = 0.72, Sc = 0.62, Du = 0.03.

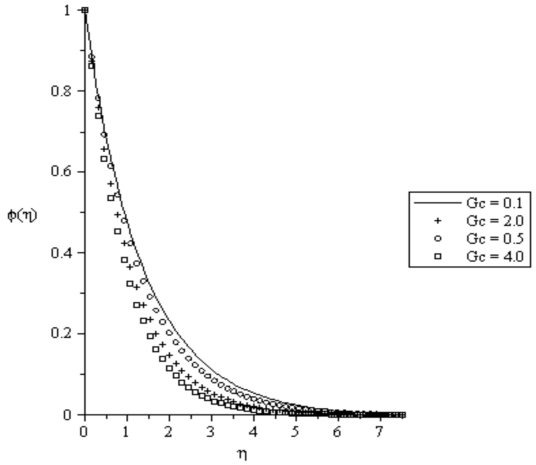

Fig. 17: Concentration profiles for Gr = F_w = Sr = γ = α = Ra = M = 0.1, Pr = 0.72, Sc = 0.62, Du = 0.03.

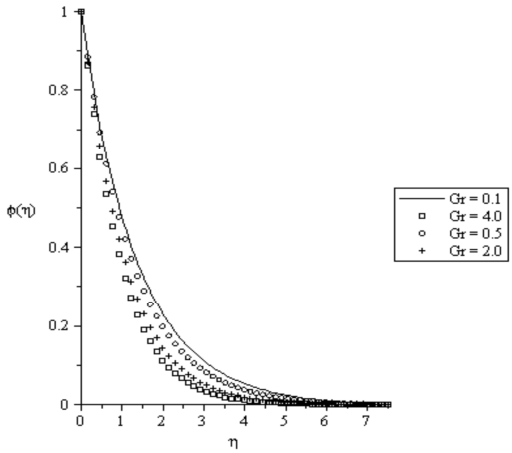

Fig. 18: Concentration profiles for Gc = F_w = Sr = γ = α = Ra = M = 0.1, Pr = 0.72, Sc = 0.62, Du = 0.03.

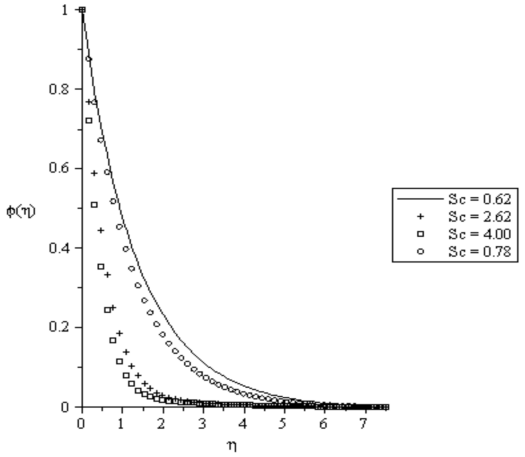

Fig. 19: Concentration profiles for Gc = Gr = F_w = Sr = γ = α = Ra = M = 0.1, Pr = 0.72, Du = 0.03.

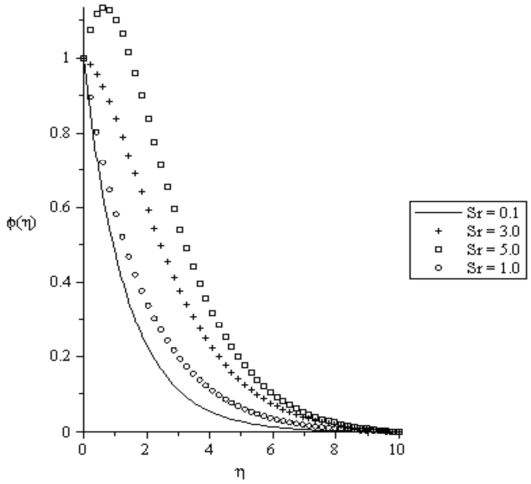

Fig. 20: Concentration profiles for Gc = Gr = F_w = γ = α = Ra = M = 0.1, Pr = 0.72, Sc = 0.62, Du = 0.03

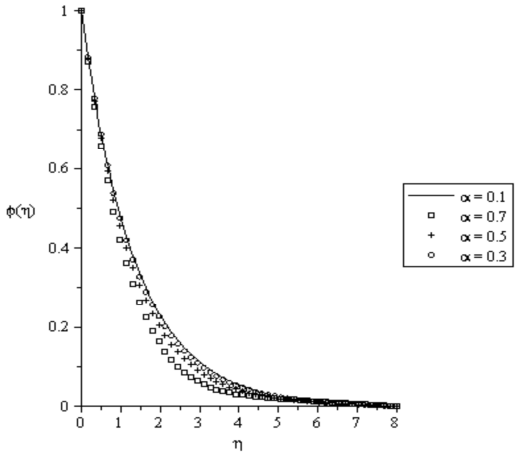

Fig. 21: Concentration profiles for Gc = Gr = F_w = γ = Ra = Sr = M = 0.1, Sc = 0.62, Du = 0.03, Pr = 0.72.

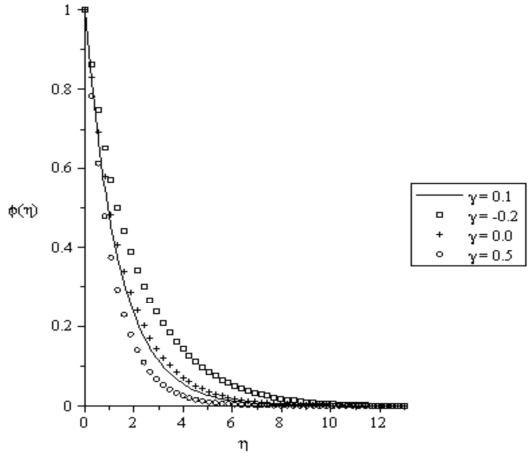

Fig. 22: Concentration profiles for Gc = Gr = F_w = α = Ra = Sr = M = 0.1, Sc = 0.62, Du = 0.03, Pr = 0.72.

Fig. 20 represents the graph of concentration profiles for various values of Soret number Sr and it was discovered that increasing this parameter the concentration boundary layer thickness increases satisfying the existing literature. Internal heat generation and the chemical reaction parameters are to decrease the concentration boundary layer thickness (Figs. 21 and 22). In Fig. 22, we established that if γ > 0 (destructive), the concentration decreases but if γ < 0 (generative), the concentration increases confirming the existing literatures.

Conclusions

We study the two-dimensional, steady, incompressible electrically conducting, laminar free convection boundary layer flow of a continuously moving vertical porous plate in a chemically reactive medium in the presence of transverse magnetic field, thermal radiation, chemical reaction, internal heat generation and Dufour and Soret effect with suction/injection. The governing nonlinear partial differential equations have been reduced to the coupled nonlinear ordinary differential equations by the similarity transformations. The problem is solved numerically using shooting techniques with the sixth order Runge-Kutta integration scheme. Comparison between the existing literature and the present study were carried out and found to be in excellent agreement.We extended the work of Ibrahim and Makinde [20] to include the magnetic field strength, the thermal radiation, Dufour and Soret numbers, internal heat generation and chemical reaction term to extend the physical application of the subject. Our results reveal among others, that the fluid velocity within the boundary layer decreases with increasing the magnetic strength and wall suction, and increases with wall injection. It was established that an increase in the wall suction enhances the boundary layer thickness and reduces the skin friction together with the heat and mass transfer rate at the moving plate surface. The temperature increases in the presence of radiation parameter and Dufour number. In addition, the chemical species concentration within the boundary layer decreases with increasing Gc, Gr, Sc and α. Soret number increases the concentration boundary layer thickness.

Acknowledgements

Prof. Olanrewaju wants to thank the Federal University Wukari, Nigeria for their financial support.

References

Alam MS & Rahman MM 2006. Dufour and Soret effects on mixed convection flow past a vertical porous flat plate with variable suction. *Nonlinear Analysis, Modelling & Control*, 11(1): 3-12.

Anwar BO, Zueco J & Takhar HS 2008. Laminar free convection from a continuously moving vertical surface in thermally-stratified non-Darcian high-porosity medium: Network numerical study. *Int. Comm. in Heat & Mass Transfer*, 35: 810-816.

Crane IJ 1970. Flow past a stretching plate. *Z. Angew. Math. Phys.*, 21(56): 1-37.

Carragher P & Crane IJ 1982. Heat transfer on a continuous stretching sheet. *Z. Angew. Math. Mech.*, 62: 564-565.

Chakrabarti A & Gupta AS 1979. Hydromagnetic flow and heat transfer over a stretching sheet. *Quart. Appl. Math*., 37: 73-78.

Danberg JE Fansler KS 1976. A nonsimilar moving wall boundary-layer problem. *Quart. Appl. Math.*, 34: 305-309.

Dutta BK 1986. Heat transfer from a stretching sheet with uniform suction and blowing. *Acta Mech*., 78: 255-262.

Catherall D & Williams S 1965. Viscous flow past a flat plate with uniform injection. *Proc. R. Soc. A.*, 284: 370-396.

Crane LJ 1970. Flow past a stretching plate. *Z. Angew. Math. Phys. (ZAMP)*, 21: 645-647.

Erickson LE, Fan LT & Fox VG 1966. Heat and mass transfer on a moving continuous flat plate with suction or injection. *Ind. Eng. Chem.*, 5: 19-25.

Gupta PS Gupta AS 1977. Heat and mass transfer on a stretching sheet with suction and blowing. *Can. J. Chem. Eng.*, 55: 744-746.

Heck A 2003. *Introduction to Maple;* 3rd Edition, Springer-Verlag.

Ingham DB & Pop I. (Eds.) 2005. Transport Phenomena in Porous Media, Vol. III, Elsevier, Oxford.

Ibrahim SY & Makinde OD 2010. Chemically reacting MHD boundary layer flow of heat and mass transfer past a moving vertical plate with suction. *Sci. Res. Essay*, 5(19): 2875–2882.

Kafoussias NG & Williams EW 1995. Thermal-diffusion and diffusion-thermo effects on mixed free-convective and mass transfer boundary layer flow with temperature dependent viscosity. *Int. J. Eng Sci.*, 33: 1369-84.

Lee SL Tsai JS 1990. Cooling of a continuous moving sheet of finite thickness in the presence of natural convection, *Int. J. Heat Mass Transfer*, 33: 457-464.

Massoudi M 2001. Local non-similarity solutions for the flow of a non-Newtonian fluid over a wedge, *Int. J. Non-Linear Mech.*, 36: 961-976.

Makinde OD 2005. Free-convection flow with thermal radiation and mass transfer past a moving vertical porous plate. *Int. Comm. in Heat & Mass Transfer*, 32: 1411-1419.

Makinde OD & Ogulu A 2008. The effect of thermal radiation on the heat and mass transfer flow of a variable viscosity fluid past a vertical porous plate permeated by a transverse magnetic field. *Chem. Engin. Comm.*, 195(12): 1575 -1584.

Nield DA & Bejan A 2006. *Convection in Porous Media*. Third ed., Springer, New York.

Olanrewaju PO 2010. Dufour and soret effects of a transient free convective flow with radiative heat transfer past a flat plate moving through a binary mixture. *Pacific J. Sci. & Tech.*, 11(1).

Sparrow EM & Cess RD 1978. *Radiation Heat Transfer*. Augmented edition, Hemisphere Publishing Corp, Washington DC.

Sparrow EM & Yu HS 1971. Local non-similarity thermal boundary-layer solutions. *J. Heat Transf. ASME,* 328-334.

Sparrow EM, Quack H & Boerner CJ 1970. Local non-similarity boundary layer solutions. *J. AIAA*, 8(11): 1936-1942.

Sparrow EM & Cess RD 1961. The effect of a magnetic field on free convection heat transfer. *Int. J. Heat Mass Transfer*, 4: 267-274.

Sakiadis BC 1961. Boundary-layer behavior on continuous solid surfaces. I. Boundary-layer equations for two-dimensional and axisymmetric flow. *AIChE J*. 7: 26-28; Boundary-layer behavior on continuous solid surfaces. II. The boundary-layer on a continuous flat surface, *AIChE J.*, 7: 221-225.

Vajravelu K 1986. Hydromagnetic flow and heat transfer over a continuous moving porous, flat surface. *Acta Mech.* 64: 179-185.

Vafai K (Ed.) 2005. *Handbook of Porous Media*. Second ed., Taylor & Francis, New York.

Vadasz P 2008. *Emerging Topics in Heat and Mass Transfer in Porous Media*. Springer, New York.

Wanous KJ & Sparrow EM 1965. Heat transfer for flow longitudinal to a cylinder with surface mass transfer. *J. Heat Transf. ASME. Ser.*, C87(1): 317-319.

Yih KA 1999. Free convection effect on MHD coupled heat and mass transfer of a moving permeable vertical surface. *Int. Commun Heat Mass Transfer*, 26(1): 95-104.